Article

Effects of Fresh Groundwater and Seawater Mixing Proportions and Salt-Freshwater Displacement on Coastal Aquifer Microbial Communities

Lin Chen [1], Meng Ma [2], Xiao Li [1,*], Kun Yu [3], Chuanshun Zhi [4], Long Cheng [1], Hongwei Ma [1], Zhuo Wang [1] and Xin Qian [5,*]

1   Shenyang Geological Survey Center, China Geological Survey, Shenyang 110034, China; chenlin01@mail.cgs.gov.cn (L.C.); chenglong@mail.cgs.gov.cn (L.C.); mahongwei@mail.cgs.gov.cn (H.M.); wangzhuo@mail.cgs.gov.cn (Z.W.)
2   State Key Laboratory of Simulation and Regulation of Water Cycles in River Basins, China Institute of Water Resources and Hydropower Research, Beijing 100048, China; mameng526@hotmail.com
3   Xi'an Geological Survey Center, China Geological Survey, Xi'an 710119, China; yukun01@mail.cgs.gov.cn
4   School of Water Conservancy and Environment, University of Jinan, Jinan 250022, China; stu_zhics@ujn.edu.cn
5   Liaoning Natural Resources Service Center, Shenyang 110033, China
*   Correspondence: lixiao@mail.cgs.gov.cn (X.L.); 13236626297@163.com (X.Q.); Tel.: +86-188-0240-9736 (X.L.); +86-138-0421-2806 (X.Q.)

Abstract: Seawater intrusion significantly affects the microbial communities within coastal aquifers. Investigating the spatial distribution of groundwater microbial communities in coastal regions is crucial for understanding seawater intrusion. The primary objective of this study is to develop a novel microbial index-based method for detecting seawater intrusion. Groundwater microbial samples were collected and sent to the laboratory in the west coastal area of Longkou City, Shandong Province. By characterizing the microbial community within the whole interval of seawater intrusion into fresh groundwater and discussing the effects of salt-freshwater displacement intensities on groundwater microbial communities, including diversity, structure, and function, using indoor domestication experiments, we reveal the response of microorganisms to the seawater intrusion process under in situ environmental conditions. The results show that the microbial community diversity is highest in environments with a seawater mixing proportion ($P_{(sm)}$) of 2.5% and lowest in those with a $P_{(sm)}$ of 75%. When considering species abundance and evolutionary processes, the microbial community structure is similar at higher $P_{(sm)}$ levels, while it is similar at lower $P_{(sm)}$ levels based on the presence or absence of species. *Tenericutes*, *Flavobacteriia*, *Rhodobacterales*, *Flavobacteriales*, *Rhodobacteraceae*, *Flavobacteriaceae*, *Cohaesibacteraceae*, and *Cohaesibacter* are significantly positively correlated with the $P_{(sm)}$. Strong salt-freshwater displacement enhanced the richness and evenness of the microbial community, whereas weak displacement showed the opposite trend. Strong displacement affects the functional profiles of the microbial community. This study effectively addressed the challenge of obtaining samples in coastal areas and also incorporated salt-freshwater displacement intensities, which can more comprehensively describe the microbial community characteristics within the groundwater of coastal aquifers.

1. Introduction

Seawater intrusion, a prevalent occurrence in coastal aquifers, poses a significant global concern. The primary hazards include the reduction in effective freshwater storage and the contamination of pumping wells [1–4], as the mixing of even 1% seawater by

volume renders freshwater non-potable [5]. Accurately detecting the extent of seawater intrusion and implementing preventative measures are thus imperative [6].

Currently, there are various mainstream methods for seawater intrusion detection and monitoring, including chemical [7–9], geophysical [10,11], and isotope [12–14] analyses. Chloride (Cl^-) is the most common indicator in chemical methods. In most countries, a Cl^- concentration of 250 mg/L is used to mark the interface between salt- and freshwater. However, because of the different background values of Cl^- in groundwater in different areas [15,16], the standards for distinguishing Cl^- are also different, and it is difficult to unify them. In geophysical prospecting, electrical resistivity tomography techniques are typically used to analyze and monitor the salt-freshwater transition interface [10,17,18]. Nevertheless, the results are inaccurate because of the great influence of groundwater salinity and geological conditions on the survey signal. Numerous isotopes have been applied to seawater intrusion. They can distinguish paleo-seawater intrusion and modern seawater intrusion, as well as identify different sources of saltwater and their spatial salinity distribution characteristics [19,20]. Many financial and material resources have been lost because of the need for the joint determination of multiple isotopes. There is a developing trend to adopt multiple indices and methods for comprehensive discrimination, and reliable results have been obtained by multi-linkage. Microbial indicators play key roles in this process [21–23]. Microbial communities are influenced by the physical and chemical properties of groundwater [24,25] and are closely related to the nutrient transport [26,27], geochemical element cycling [28–30], and pollutant degradation [31–33] in aquifers. Moreover, high-throughput sequencing technology for testing microorganisms is widely used, with a short testing time and low cost. It provides an advanced channel for a detailed and accurate understanding of bacterial diversity in groundwater.

In the early stages, some studies and analyses focusing on groundwater microbial communities within the salt-freshwater transition zone were conducted, including temporal and spatial comparisons, to identify microbial indicators that could indicate seawater intrusion [34,35]. However, there is little research on the characteristics of the groundwater microbial community in the whole interval of seawater intrusion, most of which only explores the area near the salt-freshwater transition interface. We do not know what is occurring near the coast, which makes the conclusions unrepresentative and incomprehensive. Analyses of the responses of the microbial community to specific salinity in the whole interval of seawater intrusion are thus needed.

The identification of suitable underground wells for sample collection in coastal areas is a challenging task, as many wells do not exist or are difficult to find. This has significantly hampered the comprehensive understanding of microbial community characteristics in coastal groundwater. Under natural conditions, there is always a dynamic equilibrium between saltwater and freshwater in coastal aquifers. The rise and fall of global sea levels [36,37], the amount of regional rainfall, the development degree of groundwater resources [38–40], and the permeability change in aquifer medium [41] will all cause the salt-freshwater displacement to be strong and weak, the interface will swing, and the seawater content in the groundwater of a fixed position will change. The intensity of salt-freshwater displacement directly changes the environmental conditions and then affects the microbial community of groundwater. Within our knowledge, few studies have investigated the relationship between salt-freshwater displacement and groundwater microbial communities.

To address the above issues, a whole interval of seawater intrusion into a fresh groundwater system and a salt-freshwater displacement process were established indoors. The laboratory microbial domestication experiment was conducted at a constant temperature, and microbial analysis was performed on the experimental samples. Microbial communities were obtained by sequencing bacterial 16S rDNA. The primary goals of this study were to (1) quantitatively analyze the relationship between the groundwater microbial community and seawater content in the whole interval of seawater intrusion into fresh groundwater; (2) characterize the effect of salt-freshwater displacement on the groundwater microbial

community because changes in the environment screen out more adaptable microbes; and (3) identify microbial indicators that can be used to detect seawater intrusion. We believe that the results of these experiments are very important for discussing the application of microbial indicators in the study of seawater intrusion.

2. Materials and Methods

2.1. Sampling

The sampling points were located west of Longkou City in Shandong Province. The climate of Longkou city typifies a warm–temperate sub-humid continental monsoon, characterized by a mean annual temperature of 11.7 °C. Over the past 20 years, the city has experienced an average annual rainfall of approximately 630.2 mm. Notably, approximately 72.7% of the annual precipitation occurs during the summer season. The annual evaporation is 540–580 mm. Saltwater samples were obtained from a monitoring well in the salt-freshwater transition zone for the extraction of microorganisms, and seawater near the west coast and fresh groundwater farther from the coast were used to obtain mixed water. The general indicators of the water samples collected are shown in Table S1.

Groundwater samples collected from the same location as the initial samples were used to extract microorganisms, and the microbial content of the initial samples was the same by default. The saltwater samples were vacuum-filtered through a 0.22 μm filter membrane (Millipore, Billerica, MA, USA) to collect microorganisms. Each filter membrane quantitatively filtered 2 L of the water sample (to ensure that the amount of water filtered by each filter membrane remained the same). Then, the microbial filter was placed in a 50 mL sterile centrifuge tube and stored in an ultra-low-temperature freezer at −80 °C. The seawater and fresh groundwater samples were also subjected to vacuum filtration through a 0.22 μm membrane (Millipore, Billerica, MA, USA) to filter out microorganisms. Filtered fresh groundwater and seawater samples were refrigerated at 4 °C and used to prepare the mixed water. The entire process was completed within a short period.

2.2. Experimental Material

The experiment utilized analytical-grade glucose ($C_6H_{12}O_6$) without the need for additional purification. Deionized water was used in the experiments. The instruments used in the experiment included an electronic balance (GL224-1SCN, Sartorius, Gottingen, Germany), constant-temperature incubator (303-5S, Xinnuo Instrument Group Co. Ltd., Shanghai, China), PTFE magnetic stirrer (B4, Koloke Biological & Medical Instrument Co.,Ltd., Shanghai, China), bench high-speed centrifuge (TG-18W, BIOBASE, Jinan, China), and speed-regulating multipurpose oscillator (HY-4A, Weier Experimental Supplies Co. Ltd., Suzhou, China).

2.3. Experimental Method

The experimental method was as follows:

(1) Seven groups (P1, P2, P3, P4, P5, P6, and P7) were established with different proportions of mixed water (seawater and fresh groundwater) as the domestication medium, and the corresponding glucose ($C_6H_{12}O_6$) was added to each group of mixed liquids. The specific mixing ratios and glucose contents are listed in Table 1. Taking the proportion of seawater mixing ($P_{(sm)}$) as the characteristic value of mixed water, the calculation method is as follows (without considering the density of seawater and freshwater):

$$P_{(sm)} = \frac{\text{Seawater (mL)}}{\text{Seawater (mL)} + \text{Fresh Groundwater (mL)}}$$

Table 1. Nutrient solution proportional distribution of seven groups in the full-scale seawater content experiment.

Sample	Freshwater (mL)	Seawater (mL)	$C_6H_{12}O_6$ (mg)	$P_{(sm)}$
P1	1000	0	750	0
P2	975	25	750	2.5%
P3	900	100	750	10%
P4	750	250	750	25%
P5	500	500	750	50%
P6	250	750	750	75%
P7	0	1000	750	100%

(2) The filter membrane containing microorganisms was treated to form a turbid liquid, which was placed in a 100 mL serum bottle with the corresponding proportion of the domestication medium.

(3) The serum bottles were wrapped with foil for protection against light and then placed in a 25 °C incubator for incubation.

(4) The domestication medium was changed every two days to ensure adequate nutrition.

(5) Step (4) was repeated for 180 days of acclimation domestication.

(6) Two groups of samples, P4 and P5, were selected and divided into three parts, labelled P4.1, P4.2, P4.3, P5.1, P5.2, and P5.3.

(7) P4.1 was taken as the control group, and only the original solution was replaced.

(8) A weak displacement with a gradient of $P_{(sm)}$ = 1% and strong displacement with a gradient of $P_{(sm)}$ = 5% were applied to P4.2 and P4.3, respectively. The displacement conditions for each cycle of the experiment are listed in Table 2. The medium of different proportions was replaced every two days.

Table 2. Displacement condition of one cycle of two groups in the salt-freshwater displacement experiment.

Time (Day)	P4-$P_{(sm)}$			P5-$P_{(sm)}$		
	P4.1	**P4.2**	**P4.3**	**P5.1**	**P5.2**	**P5.3**
1	25%	25%	25%	50%	50%	50%
3	25%	26%	30%	50%	51%	55%
5	25%	27%	35%	50%	52%	60%
7	25%	28%	40%	50%	53%	65%
9	25%	27%	35%	50%	52%	60%
11	25%	26%	30%	50%	51%	55%
13	25%	25%	25%	50%	50%	50%
15	25%	24%	20%	50%	49%	45%
17	25%	23%	15%	50%	48%	40%
19	25%	22%	10%	50%	47%	35%
21	25%	23%	15%	50%	48%	40%
23	25%	24%	20%	50%	49%	45%

(9) The P5 group underwent the same procedure as the P4 group. The experiment was conducted in three cycles. The experimental procedure is illustrated in Figure 1.
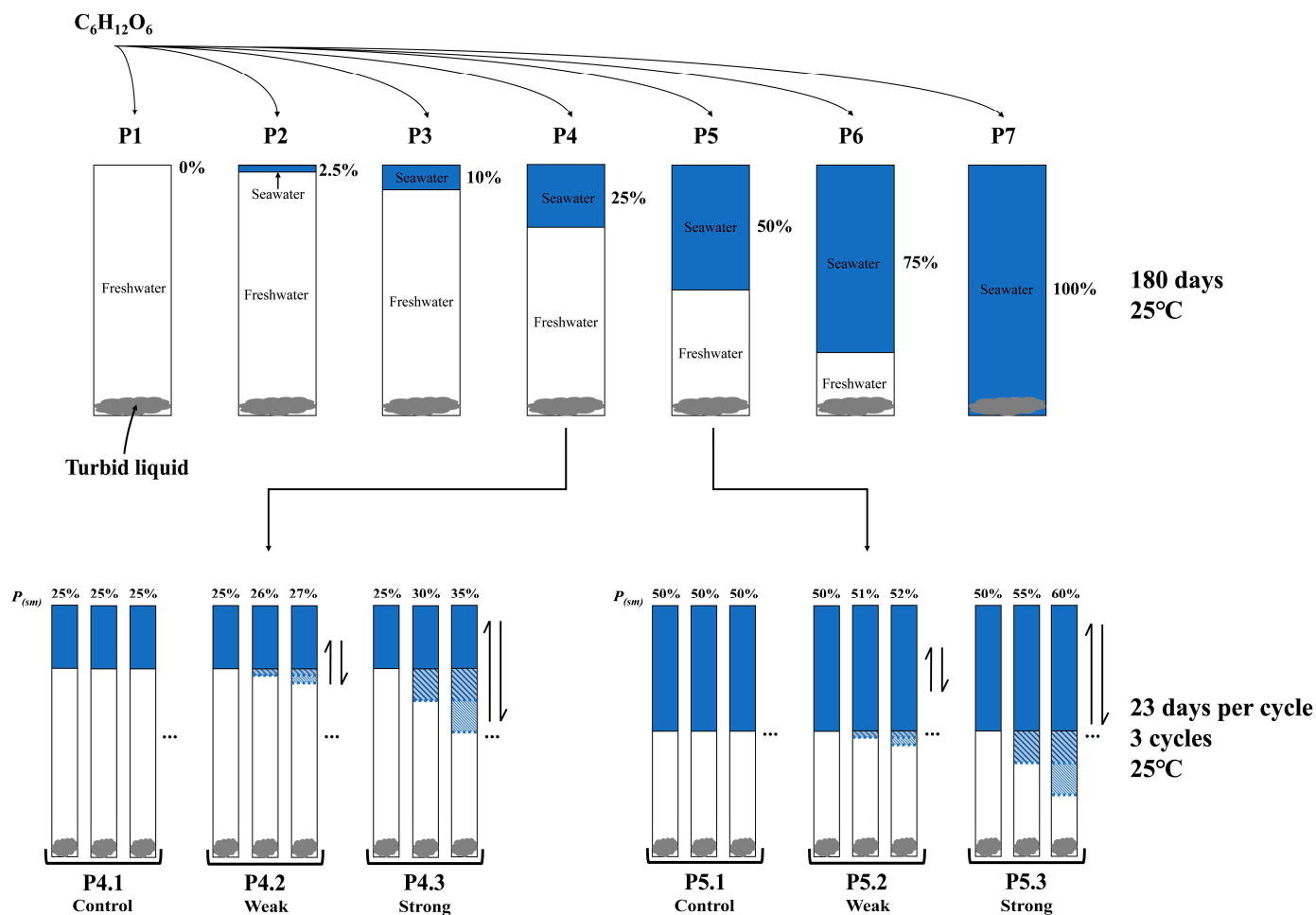
Figure 1. Schematic diagram of experimental procedure (P1: $P_{(sm)}$ = 0%, pure freshwater; P2: $P_{(sm)}$ = 2.5%, original sample; P3: $P_{(sm)}$ = 10%; P4: $P_{(sm)}$ = 25%; P5: $P_{(sm)}$ = 50%; P6: $P_{(sm)}$ = 75%; P7: $P_{(sm)}$ = 100%, pure seawater).

2.4. Microbial Analysis

All samples were centrifuged in sterile tubes at 3000 rpm for 10 min to separate the supernatant and pellet, which were then used for microbiological analysis. Total DNA was extracted using a PowerWater DNA Isolation Kit (Mobio, Solana Beach, CA, USA) in triplicate [42]. The extracted DNA was then pooled and amplified by PCR using barcoded primers 341F (5′-CCTAYGGGRBGCASCAG-3′) and 806R (5′-GGACTACNNGGGTATCTAAT-3′) [43]. The data were preprocessed, and the initial data were divided into different units according to the barcode sequence. QIIME was used to analyze the sequencing data [44–46]. The obtained reads were compared to those in the Gold database to obtain the final valid data. We set a relative number of 0.1% as the taxa threshold.

2.5. Statistical Analysis

The alpha diversity indices of the microbial community were calculated using Mothur (version 1.30.1), including Shannon, Chao 1, observed species, and phylogenetic diversity (PD) [47–49]. The similarity patterns of microbial communities were analyzed by beta diversity at different points with beta diversity indices, including Weighted Unifrac, Unweighted Unifrac, and Bray–Curtis distances using the 'vegan' package in R (version 3.6.3). The Pearson correlation analysis was used to evaluate the relationship between the proportion of seawater mixing and species diversity at a $p < 0.05$ level using SPSS.19.0. The functional prediction of the groundwater microbial community was assessed using PICRUSt to obtain a function abundance table at each level [50].

3. Results

3.1. Different Proportions of Seawater Mixing

3.1.1. Microbial Community Diversity and Structure

The alpha diversity of the microbial communities was compared using indices such as Shannon, Chao1, observed species, and PD (Table 3). According to the Shannon index, P2 (original sample) is the maximum and P6 is the minimum, indicating that the microbial community diversity is the highest in the medium with a $P_{(sm)}$ of 2.5% and the lowest in the medium with a $P_{(sm)}$ of 75%. Chao1 and the observed species index show that P3 is the minimum, whereas P7 (pure seawater) is the maximum, indicating that the richness of these two groups of samples is the minimum and maximum, respectively.

Table 3. Alpha diversity indices of seven groups in the full-scale seawater content experiment.

Sample	Diversity Indices			
	Shannon	Chao1	Observed Species	PD
P1	4.38	279	167	11.9
P2	5.00	245	164	10.6
P3	4.05	226	139	9.6
P4	4.41	279	147	9.7
P5	4.00	275	148	10.4
P6	3.49	243	162	10.8
P7	4.96	297	189	10.5

Proteobacteria are the most abundant in all samples. The relative abundance of *Proteobacteria* is highest and lowest in P2 and P7, accounting for 89.0% and 77.9% of all bacteria at the phylum level, respectively. In contrast, *Bacteroidetes* have the lowest relative abundance in P2 and the highest relative abundance in P7, accounting for 2.5% and 13.7%, respectively. *Firmicutes* (0.4–6.0%), *Cyanobacteria* (0.3–3.6%), and *Actinobacteria* (0.3–1.2%) are the most important phyla. Notably, *Spirochaetes* and *Tenericutes* are detected in P1, P4, P5, P6, and P7 but not in P2. *Verrucomicrobia* are only found in media with <10%, *Chlorobi* are only found in media with >50%, and *Gemmatimonadetes* are only detected in P1 (pure freshwater) (Figure 2A).

Figure 2B–D show the main microbial community structures at the class, order, and family levels of the seven groups of samples. *Alphaproteobacteria* (39.3–84.9%) are the dominant class of bacteria, *Rhizobiales* (15.0–46.5%) and *Rhodobacterales* (1.32–43.5%) are the dominant orders of bacteria, and there are more dominant bacteria at the family level. By comparing the composition of the microbial community, it has been observed that P3 exhibits the highest degree of similarity with P2 at the phylum and family levels. Simultaneously, P5 and P6 show similar microbial community compositions at the four levels (Figure 2).

To show the differences and trends of the seven groups of samples at the genus level more intuitively, the abundance values are presented in the form of a Bubble diagram, as shown in Figure 3. *Pseudomonas*, *Acidovorax*, *Pseudoxanthomonas*, *Sphingomonas*, *Mycoplana*, *Exiguobacterium*, *Phenylobacterium*, and *Sphingobium* are found to be in the full-scale range ($P_{(sm)}$: 0–100%). *Hydrogenophaga* exist in media with <10%; *Sporomusa* are found only in the pure freshwater environment; and *Sediminibacterium* and *Lysobacter* are found in media with <25%. *Maricaulis*, *Muricauda*, and *Winogradskyella* are found in media with >25%. *Diaphorobacter*, *Azorhizobium*, and *Asticcacaulis* are present in environments with $P_{(sm)} < 50\%$, whereas *Vibrio*, *Nautella*, and *Balneola* are found in environments with $P_{(sm)} > 50\%$.
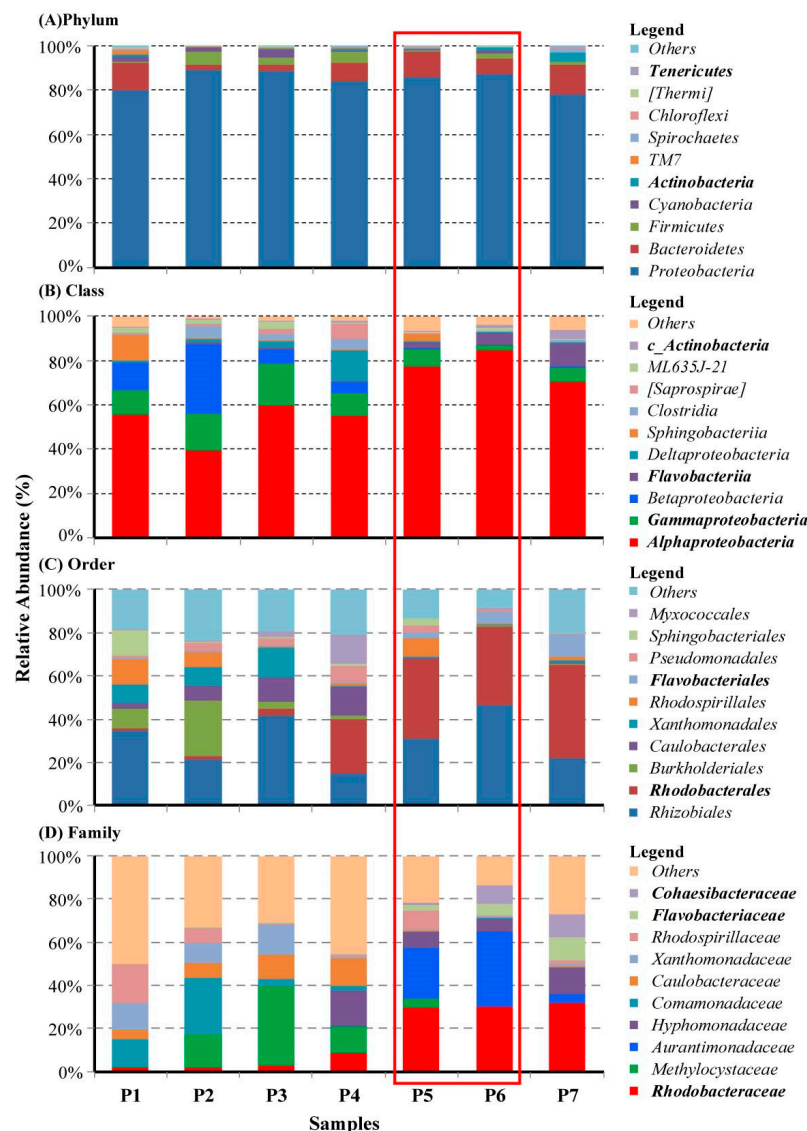
Figure 2. Bar charts representing relative abundance of the dominant bacterial communities from the full-scale seawater content experiment classified at the (**A**) phylum, (**B**) class, (**C**) order, and (**D**) family level; P5 and P6 are similar in microbial community composition (the bacteria in bold are correlated with $P_{(sm)}$, as shown in Table 4).

Table 4. The Pearson correlation analysis of microbial communities of five levels and $P_{(sm)}$ in the full-scale seawater content experiment (top 10 is selected for each level).

Level	Species	$P_{(sm)}$	Level	Species	$P_{(sm)}$
Phylum	*Proteobacteria*	−0.36	Order	*Rhodospirillales*	−0.45
Phylum	*Bacteroidetes*	0.49	Order	*Flavobacteriales*	0.95 **
Phylum	*Firmicutes*	−0.42	Order	*Pseudomonadales*	−0.47
Phylum	*Cyanobacteria*	−0.61	Order	*Sphingobacteriales*	−0.44
Phylum	*Actinobacteria*	0.78 *	Order	*Myxococcales*	−0.23
Phylum	*TM7*	−0.54	Family	*Rhodobacteraceae*	0.94 **
Phylum	*Spirochaetes*	0.68	Family	*Methylocystaceae*	−0.53
Phylum	*Chloroflexi*	−0.14	Family	*Aurantimonadaceae*	0.57
Phylum	*[Thermi]*	−0.59	Family	*Hyphomonadaceae*	0.58
Phylum	*Tenericutes*	0.93 **	Family	*Comamonadaceae*	−0.61
Class	*Alphaproteobacteria*	0.77 *	Family	*Caulobacteraceae*	−0.61
Class	*Gammaproteobacteria*	−0.78 *	Family	*Xanthomonadaceae*	−0.73

Table 4. *Cont.*

Level	Species	$P_{(sm)}$	Level	Species	$P_{(sm)}$
Class	*Betaproteobacteria*	−0.68	Family	*Rhodospirillaceae*	−0.45
Class	*Flavobacteriia*	0.95 **	Family	*Flavobacteriaceae*	0.95 **
Class	*Deltaproteobacteria*	−0.25	Family	*Cohaesibacteraceae*	0.92 **
Class	*Sphingobacteriia*	−0.44	Genus	*Pleomorphomonas*	−0.53
Class	*Clostridia*	−0.50	Genus	*Martelella*	0.57
Class	*[Saprospirae]*	−0.32	Genus	*Hyphomonas*	0.56
Class	*ML635J-21*	−0.61	Genus	*Phenylobacterium*	−0.36
Class	*c_Actinobacteria*	0.76 *	Genus	*Cohaesibacter*	0.92 **
Order	*Rhizobiales*	0.05	Genus	*Hydrogenophaga*	−0.62
Order	*Rhodobacterales*	0.93 **	Genus	*Pseudomonas*	−0.25
Order	*Burkholderiales*	−0.61	Genus	*Vogesella*	−0.88 **
Order	*Caulobacterales*	−0.61	Genus	*Acidovorax*	−0.54
Order	*Xanthomonadales*	−0.73	Genus	*Clostridium*	−0.60

Note: ** indicates significant differences at $p < 0.01$; * indicates significant differences at $p < 0.05$.
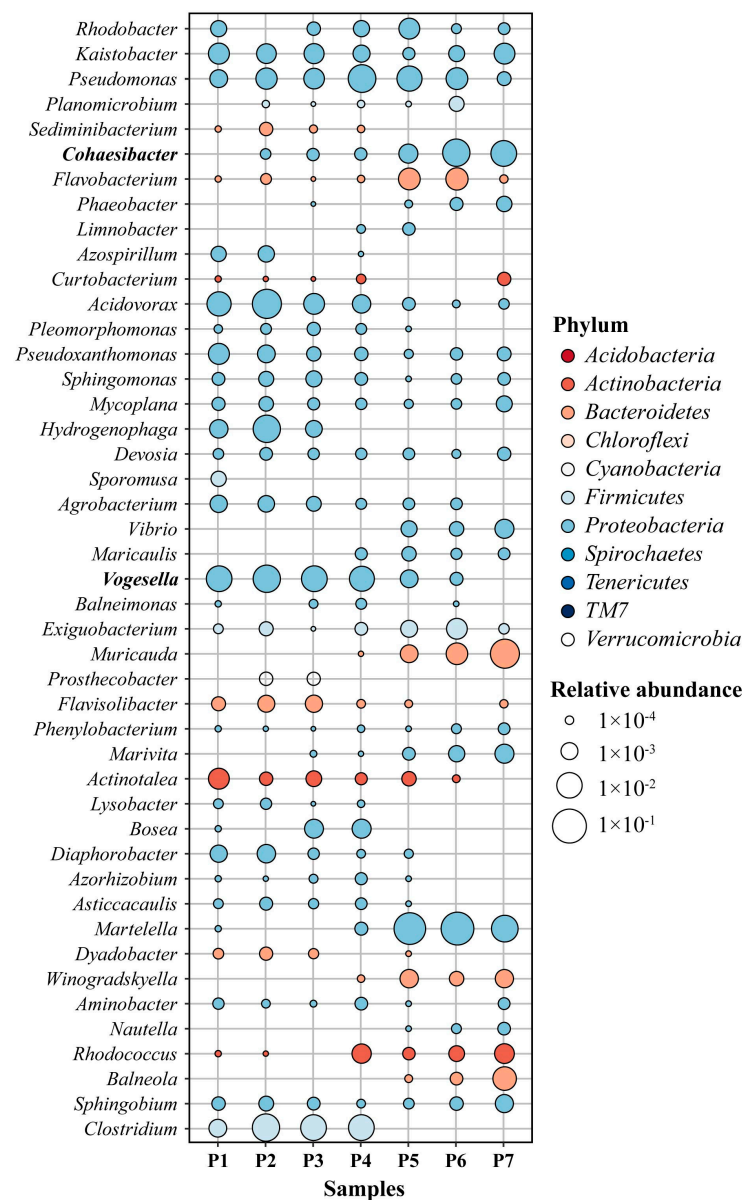

Figure 3. Structural differences in microbial communities at the genus level of the full-scale seawater content experiment (the bacteria in bold are correlated with $P_{(sm)}$, as shown in Table 4).

3.1.2. Relationship between Microbial Community and $P_{(sm)}$

The Pearson correlation analysis was performed on the microbial community abundance of five levels (phylum, class, order, family, genus) and $P_{(sm)}$, and the results are shown in Table 4. *Tenericutes*, *Flavobacteriia*, *Rhodobacterales*, *Flavobacteriales*, *Rhodobacteraceae*, *Flavobacteriaceae*, *Cohaesibacteraceae*, and *Cohaesibacter* are significantly positively correlated with $P_{(sm)}$ ($p < 0.01$), whereas *Vogesella* are significantly negatively correlated with $P_{(sm)}$ ($p < 0.01$). *Actinobacteria*, *Alphaproteobacteria*, *Gammaproteobacteria*, and *c_Actinobacteria* are positively correlated with $P_{(sm)}$ ($p < 0.05$).

3.1.3. Statistical Analysis

Principal coordinate analysis (PCoA) was performed to visually identify similarities and differences among the seven groups of samples [51,52]. As shown in Figure 4, P5, P6, and P7 cluster together in the Bray_Curtis and Weighted_Unifrac matrices, indicating that their microbial community structures are similar when considering species abundance and evolutionary progress. P1, P2, and P3 cluster together in the Unweighted_Unifrac matrices, indicating that their microbial community structures are similar when only the presence or absence of species is considered.
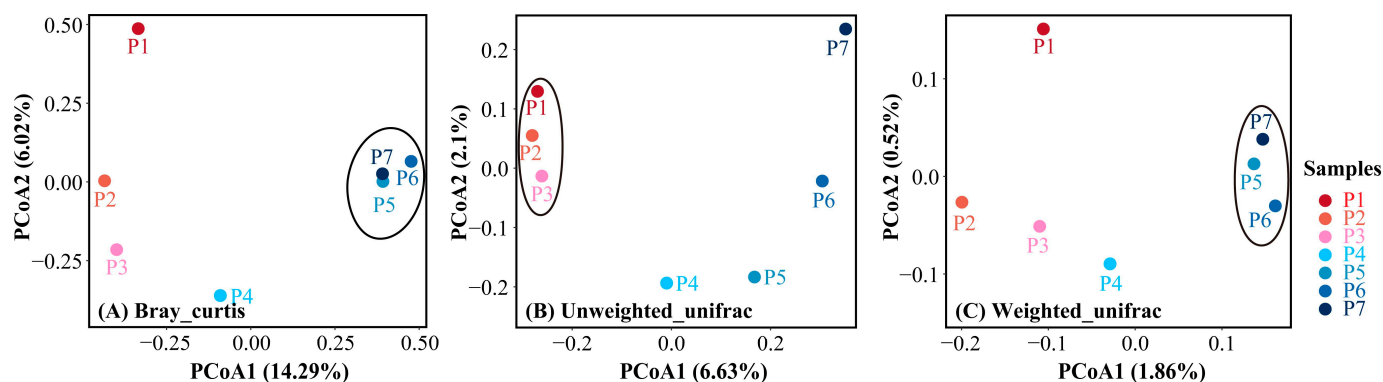

Figure 4. Principal coordinates analysis results with (**A**) Bray_Curtis, (**B**) Unweighted_UniFrac, and (**C**) Weighted_UniFrac matrices of the full-scale seawater content experiment.

3.1.4. Functional Profiles of Microbial Community

Combined with the 16S rDNA sequencing data, PICRUSt is used to predict the microbial functions of the seven groups of samples and to explore the relationship between the functional profiles and $P_{(sm)}$. There are seven and forty-one gene clusters at level 1 and level 2 of the functional gene classification of the microbial community, respectively (Figure S1). At level 1, the functional features are divided into seven categories: cellular processes, environmental information processing, genetic information processing, human diseases, metabolism, organismal systems, and unclassified. At level 2, membrane transport, amino acid metabolism, and carbohydrate metabolism dominate. The Pearson correlation analysis was performed for the 41 gene clusters at level 2 with $P_{(sm)}$ in Table S2. Cancers and signal transduction are significantly correlated with $P_{(sm)}$ ($p < 0.01$): the former is positively correlated, and the latter is negatively correlated. Amino acid metabolism, cardiovascular diseases, cell communication, the metabolism of cofactors and vitamins, the nervous system, and neurodegenerative diseases are positively correlated with $P_{(sm)}$ ($p < 0.05$). Cell motility and cellular processes and signaling are negatively correlated with $P_{(sm)}$ ($p < 0.05$).

3.2. Different Intensities of Salt-Freshwater Displacement

3.2.1. Microbial Community Diversity and Structure

The alpha diversity of the two groups of samples was analyzed, and four indices were calculated, as shown in Table 5. The Shannon values and Chao1 values of the P4 experimental group show that P4.3 is obviously improved compared with P4.1, while P4.2

is almost unchanged or slightly decreased; the trend of the P5 experimental group is the same as that of P4. The PD values and observed species are correlated tightly with $R^2 = 0.97$ ($p < 0.01$), which indicates that the microbial communities are evenly distributed in the phylogenetic tree [21].

Table 5. Alpha diversity indices of two groups in the salt-freshwater displacement experiment.

Group	Sample	Diversity Indices			
		Shannon	Chao1	Observed Species	PD
P4	P4.1	2.09	42	16	2.06
	P4.2	2.00	43	20	2.56
	P4.3	3.13	69	19	2.07
P5	P5.1	0.33	9	6	0.90
	P5.2	0.04	2	2	0.53
	P5.3	2.68	50	19	1.98

Figure 5 shows the community structures at the phylum, class, order, and family levels for the two groups of samples. *Proteobacteria* (88.9–99.8%) are the most abundant bacterial phylum in all samples. The relative abundance of Bacteroidetes (1.3%) in P4.3 is higher than that in P4.1 (0.5%) and P4.2 (0.2%), and the other phyla are low (Figure 5A). In all samples, *Alphaproteobacteria* (86.9–99.9%) are the most abundant class, followed by *Deltaproteobacteria* (2.5 ± 3.9%), *Betaproteobacteria* (0.6% ± 0.8%), and *Gammaproteobacteria* (0.6 ± 0.7%); they are all the proteobacterial subdivisions. The relative abundance of *Alphaproteobacteria* is P4.1 > P4.2 > P4.3, while that of *Deltaproteobacteria* is the opposite in the P4 experimental group. *Betaproteobacteria* and *Gammaproteobacteria* in P4.2 are significantly higher than in P4.1 and P4.3. In the P5 experimental group, *Alphaproteobacteria* in P5.2 are dominant, and there are more kinds of bacteria in P5.3 than in P5.1 and P5.2, including *Bacteroidia* and *Sphingobacteriia* (Figure 5B). At the order level, *Rhodospirillales* (43.6 ± 26.1%) are dominant, followed by *Rhizobiales* (23.1 ± 16.4%), *Caulobacterales* (16.0 ± 8.5%), *Rhodobacterales* (6.9 ± 5.0%), *Myxococcales* (4.9 ± 4.4%), *Sphingomonadales* (2.2 ± 2.2%), and *Neisseriales* (0.7 ± 0.8%) in the P4 experimental group. Among them, the relative abundance of *Rhodospirillales* and *Neisseriales* is as follows: P4.2 > P4.1 > P4.3; that of *Rhizobiales* and *Rhodobacterales* is as follows: P4.3 > P4.1 > P4.2; and that of *Myxococcales* and *Sphingomonadales* is as follows: P4.3 > P4.2 > P4.1. The results of the order level of P5.2 are consistent with those of the class level, *Rhodobacterales* are dominant, and there are many kinds of bacterial orders in P5.3 (Figure 5C).

The distribution of the main families is shown in Figure 5D. The four families with a relative abundance greater than 1% are all from *Alphaproteobacteria* in the P4 experimental group, including *Rhodospirillaceae*, *Caulobacteraceae*, *Methylocystaceae*, and *Rhodobacteraceae*. Besides the common abundant families, several families of bacteria are only abundant in specific samples, such as *Hyphomicrobiaceae* (9.7%) of P4.1, *Cohaesibacteraceae* (4.7%) of P4.2, and *Hyphomonadaceae* (6.6%), *Sphingomonadaceae* (5.4%), and *Rhizobiaceae* (3.5%) of P4.3. There are seven families with a relative abundance of over 1% in P5.3, matching the P4 experimental group, all of which are affiliated with *Alphaproteobacteria*. The *Rhodobacteraceae* family predominates in P4.1 and P4.2, constituting 97.2% and 99.3% of the total families and categories, respectively. Figure 6 shows the distribution of microbial communities at the genus level, with both sample groups combined for analysis. Genera exhibiting a high relative abundance include *Novispirillum*, *Pleomorphomonas*, *Phenylobacterium*, and *Martelella*. Unclassified genera from the *Rhodobacterales* order are also abundant in both experiment groups.
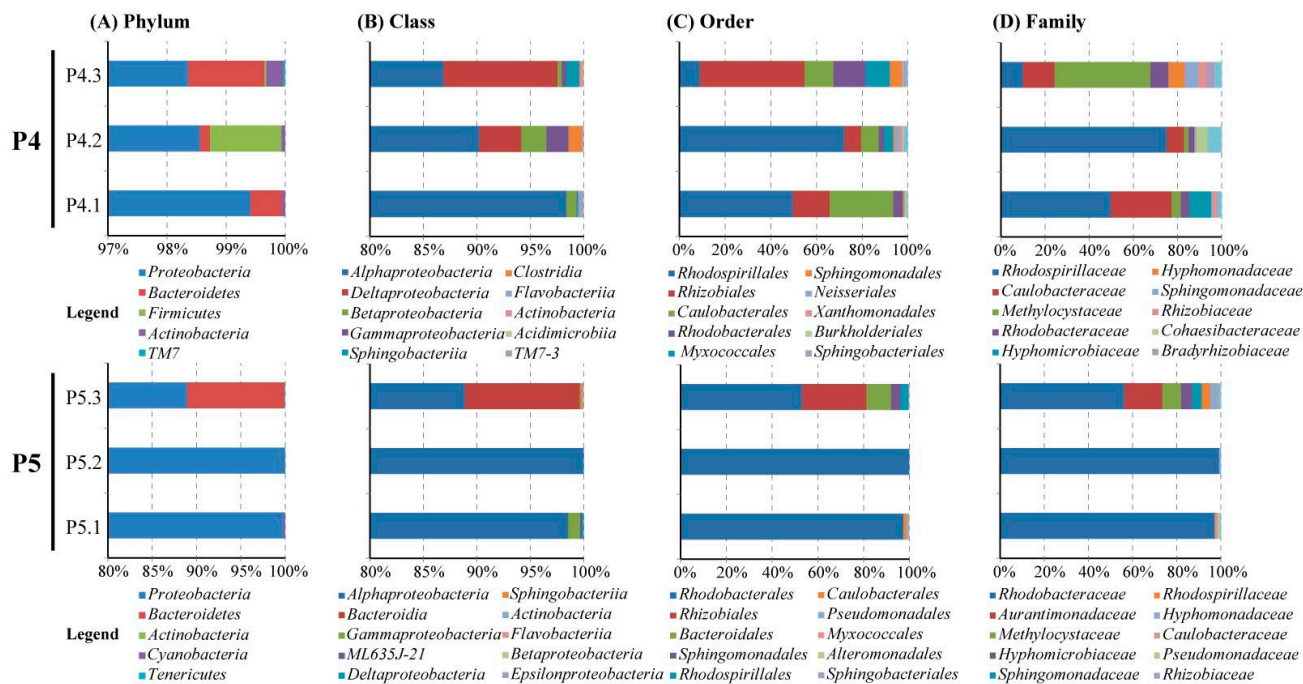
Figure 5. Bar charts representing relative abundance of the dominant bacterial communities in P4 and P5 samples from the salt-freshwater displacement experiment classified at the (**A**) phylum, (**B**) class, (**C**) order, and (**D**) family level.

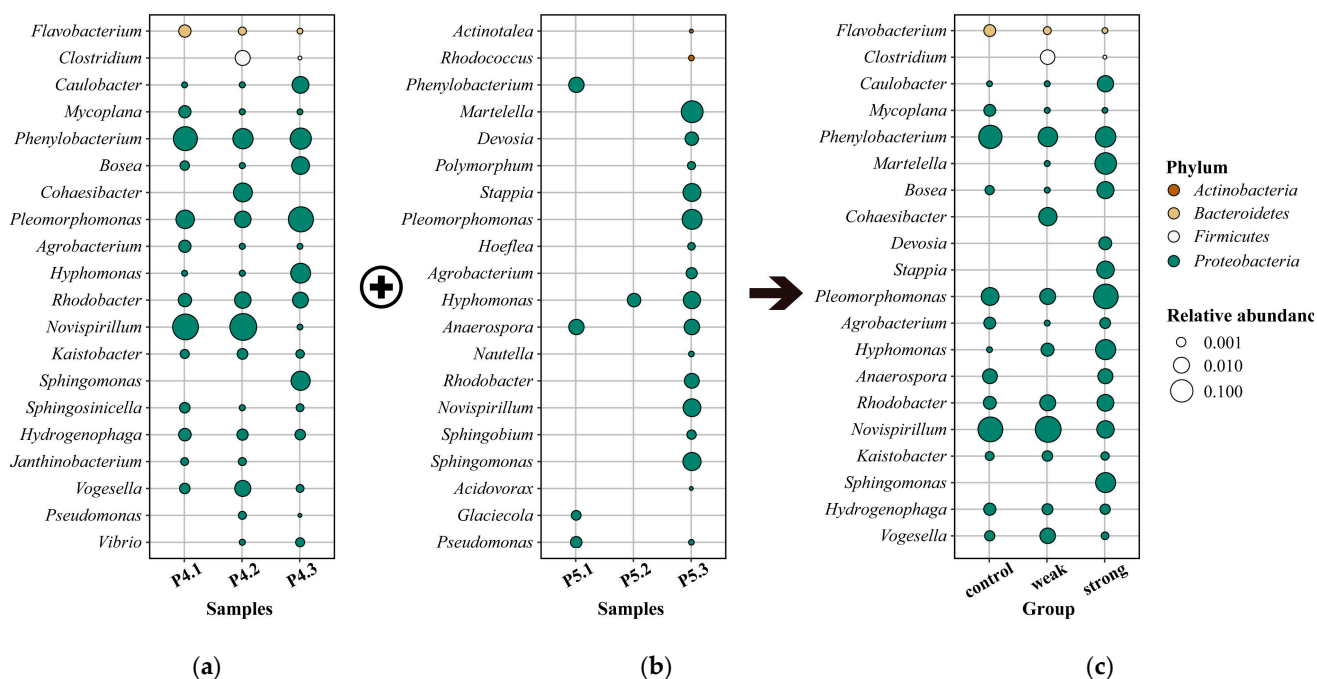(**a**)   (**b**)   (**c**)

Figure 6. Structural differences in microbial communities at the genus level of the salt-freshwater displacement experiment: (**a**) P4 group; (**b**) P5 group; and (**c**) combined group.

3.2.2. Statistical Analysis

Three matrix calculation methods were used to analyze the differences between the microbial community groups of the samples and to explore the effects of different intensities of salt-freshwater displacement on the distribution of microbial community structures (Figure 7). In the Bray_Curtis and Weighted_Unifrac matrices, the P4.1 and P4.2 and P5.1 and P5.2 groups of microbial communities are clustered together, whereas the P4.3 and

P5.3 groups are scattered. In the Unweighted_Unifrac matrix, the microbial communities of the P4.3 and P5.3 groups are clustered together, while the microbial communities of the P4.1, P4.2, P5.1, and P5.2 groups are scattered.
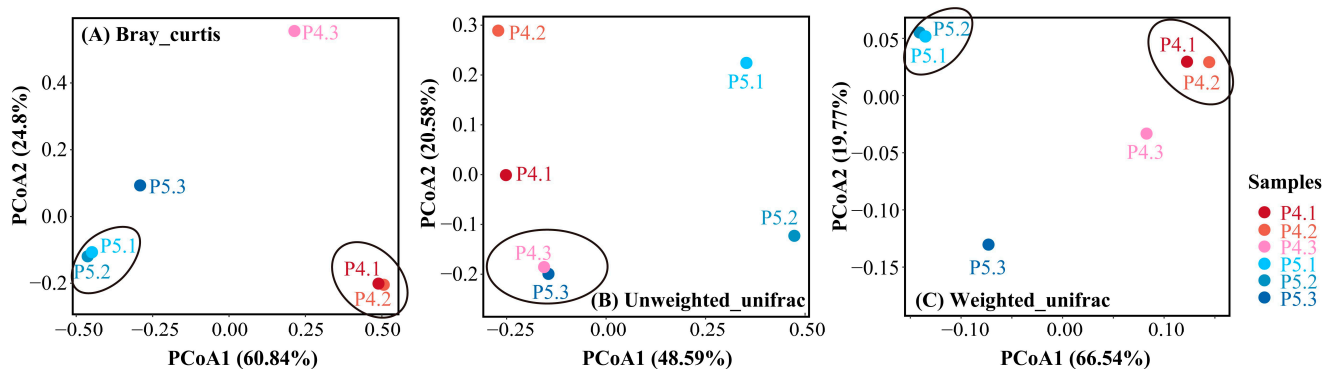

Figure 7. Principal coordinates analysis results with (**A**) Bray_Curtis, (**B**) Unweighted_UniFrac, and (**C**) Weighted_UniFrac matrices of the salt-freshwater displacement experiment.

3.2.3. Functional Profiles of Microbial Community

The predicted microbial functions of the samples are presented in Figure 8. This result illustrates the differences in the functional genes of the microbial community among the strong displacement, weak displacement, and control groups. Based on the results, it can be concluded that weak displacement has a minimal impact on the functional profiles of the microbial community, with both P4 and P5 experimental groups showing the same results. In contrast, a significant influence is observed for strong displacement on the functional profiles. Specifically, strong displacement notably alters the distribution profiles of microbial functions in the P4 experimental group, resulting in significant differences among P4.3, P4.1, and P4.2. However, the changes in functional properties are not significant in the P5 experimental group.
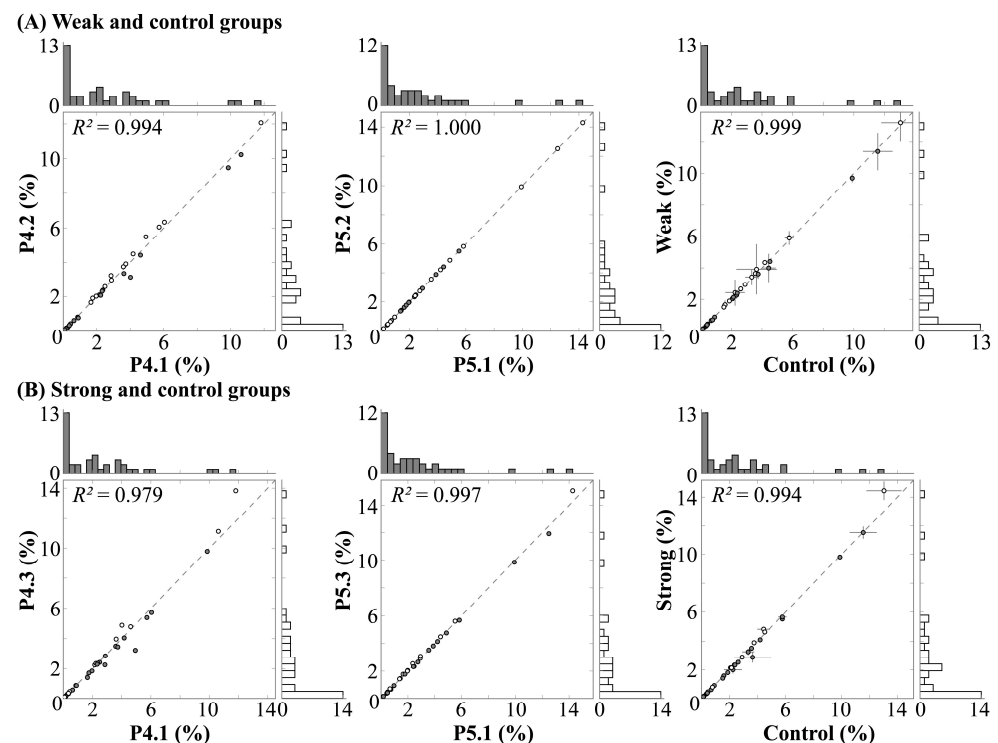

Figure 8. Scatter plot analysis of functional prediction of microbial community of the salt-freshwater displacement experiment at KEGG level 2.

4. Discussion

4.1. Characteristics of Groundwater Microbial Community along the Whole Interval of Seawater Intrusion into Fresh Groundwater

Seawater intrusion leads to the convergence of marine and freshwater microorganisms, generating a new ecological community. To identify seawater intrusion, it is crucial to analyze this new community and discuss its relationship with environmental factors. We analyzed the distribution of microbial communities at different seawater content locations (Figures 2 and 3), which is the focus of our research.

The microbial diversity of P2 (original sample) exhibits the highest value among the other groups, indicating that environmental stability is an important condition for the growth of numerous microorganisms, while rapid environmental changes can be detrimental to individual microbial growth. The microbial community richness of P1 (pure freshwater) and P7 (pure seawater) are higher in the domestication experiment, suggesting that a single environment had little influence on microorganisms and is convenient for their growth [53]. Although salinity is acknowledged as a significant factor shaping microbial community richness and evenness [54,55], our experiment reveals that its influence on bacterial community diversity is insignificant.

Proteobacteria are the most abundant and largest species at the phylum level in all samples, with a low relative abundance in P1 (pure freshwater) and P7 (pure seawater). Notably, *Bacteroides* is highly represented in P7, which is consistent with the previous research results of field sampling data [21,56] and indirectly indicates the reliability of the experiment. P5 and P6 exhibit similar microbial community structures (Figure 2), indirectly indicating that the locations at $P_{(sm)}$ of 50% and 75% are very close. Despite differences in seawater content, the groundwater microorganisms are less affected due to their similar geographical location. Through the analysis of the microbial community at the genus level, we identified microorganisms adapted to different environments (Figure 3). *Hydrogenophaga* is exclusively enriched in groundwater with low salinity yet absent in the areas near the coastal zone. Some studies have demonstrated that *Hydrogenophaga* is more dependent on an oxidizing groundwater environment [48] and is generally enriched in freshwater environment [34,35], indicating that a low content of *Hydrogenophaga* corresponds to high degrees of seawater intrusion.

The result of PCoA shows that when the groundwater salinity is within a relatively low range ($P_{(sm)}$ < 10%), only the microbial species remain unaffected. In contrast, when salinity levels are comparatively high ($P_{(sm)}$ > 50%), the impact on microbial richness is not significant, which is consistent with previous research findings [57,58]. To analyze the interface between saltwater and freshwater through microbial indicators, it is crucial to give due consideration to changes in microbial abundance. This is because the interface typically occurs at low salinity levels.

4.2. Relationship between Microbial Communities and $P_{(sm)}$

Representative bacteria were screened out by the correlation between microbial community abundance, functional profiles, and $P_{(sm)}$, which can be used to detect seawater intrusion (Table 4 and Table S2). It was found that there was a significant correlation between a variety of bacteria and $P_{(sm)}$. At the phylum level, a positive correlation between the relative abundance of *Actinobacteria* and salinity was identified. However, *Actinobacteria* naturally inhabit both marine and fresh groundwater environments [59]. To delve into the role of *Actinobacteria* in the context of seawater intrusion, we believe it is essential to focus more on the distribution and dynamics of marine *Actinobacteria* within groundwater ecosystems. In this study, we have not yet distinguished their initial sources—marine or fresh groundwater environments. At the class level, an increase in *Alphaproteobacteria* and *Flavobacteriia* is found with increasing $P_{(sm)}$, which is consistent with the results of previous studies [60,61]. *Gammaproteobacteria* were also identified as a class which increases with salinity [61,62], which is contrary to our conclusion. This is probably due to the narrow range of salinity they considered, and our upper limit of salinity is close to seawater.

Some studies found that *Betaproteobacteria* decreased with salinity in some regions [51,63]. Although there is no obvious correlation, the trend is the same in this experiment. At the family level, *Rhodobacteraceae* are often identified in estuaries and open oceans [64,65]. *Flavobacteriaceae* also exist in marine environments [66]. Unno et al. explored *Flavobacteriaceae* and *Rhodobacteraceae* as microbial indicators of seawater intrusion when describing the effects of seawater intrusion on groundwater microbial community [67]. We determined a significant positive correlation between two families of bacteria and $P_{(sm)}$ through indoor domestication experiments, thereby proving that they can be used to detect seawater intrusion. *Cohaesibacteraceae* are formed by strains from coastal marine environments [68] and contain only a single genus, *Cohaesibacter* [69]. From the results of the relationship between *Cohaesibacteraceae*, *Cohaesibacter*, and $P_{(sm)}$, it can be inferred that they invaded the groundwater environment from the seawater environment and survived. However, at present, there is relatively little discussion about them, and whether they can be used as new indicators of seawater intrusion needs to be further explored.

Cancers, cardiovascular diseases, and neurodegenerative diseases are positively correlated with $P_{(sm)}$, indicating that groundwater with a higher salt content is undrinkable [70] and even causes diseases in the human body. There is a relationship between the metabolic functional genes involved in amino acid metabolism and the metabolism of cofactors and vitamins and $P_{(sm)}$, implying the potential effect of salinity on the metabolic functions of microbial communities [71]. Functional genes responsible for the signal transduction mechanism, which is vital for microbes in dealing with the changes in environmental conditions [72], are negatively correlated with $P_{(sm)}$, and this indicates the response of microbial communities to salinity. Since salinity could cause signaling molecules to inhibit biofilm formation [73–76], it may have prevented the formation of microbial community functions in signal transduction. The above results show that the functional genes of bacteria can be used as an auxiliary index to detect seawater intrusion.

4.3. Effects of Salt-Freshwater Displacement on Groundwater Microbial Community

Salt-freshwater displacement affects the diversity of the microbial community. Strong displacement increases the richness and evenness, whereas weak displacement decreases them, indicating that drastic environmental changes have a significant impact on microbial diversity [77,78]. *Rhodobacterales* are the most abundant order of bacteria, and strong displacement decreases their relative abundance, whereas weak displacement increases their relative abundance. It is reported that *Rhodobacterales* are a widespread, abundant, and metabolically versatile order of bacteria found in oceans worldwide [79,80]. They are mainly associated with aerobic anoxygenic photosynthetic activity and are actively involved in organic carbon degradation [81]. The role of *Rhodobacterales* in promoting genetic exchange in natural environments makes them even more compelling microorganisms [79], and *Rhodobacterales* show strong seasonal variations in abundance [82]. However, there are many environmental factors that change with the seasons, and the root cause may be the intensity of salt-freshwater displacement, as mentioned above. *Alphaproteobacteria* and *Rhodospirillaceae* also show the same trend.

Figure 7 shows the effects of the intensity of salt-freshwater displacement on the distribution of microbial communities. The microbial communities of the control and weak displacement groups are similar in structure when species abundance and evolution process are considered and only the presence or absence of species is considered, and strong displacement makes the microbial community structure similar regardless of the original environment. Salt-freshwater displacement also affects the functional characteristics of microbial communities. The lower the $P_{(sm)}$ in the original environment, the greater the impact of strong displacement on microbial function. In other words, the more strongly the environmental microbes are perturbed, the more significant the changes in their functional properties [83].

We do not divide the microbial communities into rare and dominant taxa [21], which may cause some structural bias because the intensity of displacement changes is subtle

in itself, and exploring the response of rare microorganisms in this process may be more instructive for understanding the biogeochemical processes of coastal groundwater.

4.4. The Shortcomings of the Application of Microbial Indicators in Seawater Intrusion

Using microbial indicators to detect seawater intrusion, while valuable, also has several inherent shortcomings. This is primarily reflected in the following aspects: Firstly, the microbial diversity in areas affected by seawater intrusion is exceedingly complex, and current analytical technologies may not be fully capable of capturing the entirety of microbial communities, particularly those that are rare or difficult to cultivate [15,84]. Secondly, there is interference from environmental factors. Environmental factors in areas affected by seawater intrusion, such as salinity, temperature, and pH, may influence the distribution and activity of microorganisms. These factors could potentially conflict with the stability and reliability of microbial indicators [21,34,35]. Thirdly, there are limitations in our understanding of microbial ecological functions. While current research has made strides in studying the structure of microbial communities, our knowledge of their ecological functions and the mechanisms by which they operate remains relatively constrained [85,86]. This gap in understanding can limit the comprehensive interpretation of microbial activity and its implications in the context of seawater intrusion. Lastly, there is the issue of the generalizability of microbial indicators. While certain indicators may be effective in specific areas where seawater intrusion is occurring, they may not be universally applicable to all types of coastal environments. Various coastal areas have unique factors that influence the intrusion of seawater, including the speed, mode, and pathways [6]. All of these factors contribute to differences in microbial communities.

This variability underscores the need for a more complete approach that considers the unique characteristics of each coastal ecosystem when applying microbial indicators as a tool for environmental assessment and monitoring.

5. Conclusions

This study provides the first insights into the groundwater microbial community in the whole interval of seawater intrusion into fresh groundwater and evaluates the effect of salt-freshwater displacement on the microbial community through indoor domestication experiments. The results showed that the diversity of the microbial community was the highest and lowest in environments with a $P_{(sm)}$ of 2.5% and 75%, respectively. According to the PCoA, when considering the species abundance and evolution process, the microbial community structure was similar at $P_{(sm)}$ values of 50%, 75%, and 100%. When considering the presence or absence of species, the microbial community structure was similar at $P_{(sm)}$ values of 0%, 2.5%, and 10%. According to the Pearson correlation analysis, *Tenericutes*, *Flavobacteriia*, *Rhodobacterales*, *Flavobacteriales*, *Rhodobacteraceae*, *Flavobacteriaceae*, *Cohaesibacteraceae*, and *Cohaesibacter* were significantly positively correlated with $P_{(sm)}$. Although the relative abundance and function of many bacteria are associated with salinity, they cannot all serve as indicators of seawater intrusion due to their susceptibility to other factors. A comprehensive consideration of species abundance, evolution process, and the presence or absence of species is essential. *Flavobacteriaceae* and *Rhodobacteraceae* could serve as microbial indicators for assessing seawater intrusion, while further exploration is needed for *Tenericutes* and *Cohaesibacteraceae*. Environmental stability is a crucial prerequisite for the growth of many microorganisms, and rapid environmental changes can hinder the growth of individual microorganisms. The salt-freshwater displacement alters the diversity, distribution, and function of the microbial community. Strong displacements enhance the richness and evenness of the microbial community, whereas weak displacements exhibit the opposite trend. Strong displacement impacted the functional characteristics of the microbial community, with a lower salinity environment exhibiting a greater impact. These findings extend our understanding of microbial community dynamics during seawater intrusion and pave the way for novel detection methods of seawater intrusion. Subsequent studies are expected to broaden the experimental horizons, concentrating on the refinement of fresh

groundwater and seawater mixing proportions and the enrichment of key environmental factors. These methodological enhancements are poised to yield a more precise depiction of the ambient conditions prevalent in the designated study area.

References

1. Balasubramanian, M.; Sridhar, S.G.D.; Ayyamperumal, R.; Karuppannan, S.; Gopalakrishnan, G.; Chakraborty, M.; Huang, X. Isotopic signatures, hydrochemical and multivariate statistical analysis of seawater intrusion in the coastal aquifers of Chennai and Tiruvallur District, Tamil Nadu, India. *Mar. Pollut. Bull.* **2022**, *174*, 113232. [CrossRef] [PubMed]
2. Barlow, P.M.; Reichard, E.G. Saltwater intrusion in coastal regions of North America. *Hydrogeol. J.* **2010**, *18*, 247–260. [CrossRef]
3. Sappa, G.; Ergul, S.; Ferranti, F.; Sweya, L.N.; Luciani, G. Effects of seasonal change and seawater intrusion on water quality for drinking and irrigation purposes, in coastal aquifers of Dar es Salaam, Tanzania. *J. Afr. Earth Sci.* **2015**, *105*, 64–84. [CrossRef]
4. Werner, A.D.; Bakker, M.; Post, V.E.A.; Vandenbohede, A.; Lu, C.H.; Ataie-Ashtiani, B.; Simmons, C.T.; Barry, D.A. Seawater intrusion processes, investigation, and management: Recent advances and future challenges. *Adv. Water Resour.* **2013**, *51*, 3–26. [CrossRef]
5. Chang, Y.W.; Hu, B.X.; Xu, Z.X.; Li, X.; Tong, J.X.; Chen, L.; Zhang, H.X.; Miao, J.J.; Liu, H.W.; Ma, Z. Numerical simulation of seawater intrusion to coastal aquifers and brine water/freshwater interaction in south coast of Laizhou Bay, China. *J. Contam. Hydrol.* **2018**, *215*, 1–10. [CrossRef] [PubMed]
6. Cao, T.Z.; Han, D.M.; Song, X.F. Past, present, and future of global seawater intrusion research: A bibliometric analysis. *J. Hydrol.* **2021**, *603*, 126844. [CrossRef]
7. Daniele, L.; Tardani, D.; Schmidlin, D.; Quiroga, I.; Cannatelli, C.; Somma, R. Seawater intrusion and hydrogeochemical processes in the Ischia Island groundwater system. *J. Geochem. Explor.* **2022**, *234*, 106935. [CrossRef]
8. Dhakate, R.; Ratnalu, G.V.; Sankaran, S. Hydrogeochemical and isotopic study for evaluation of seawater intrusion into shallow coastal aquifers of Udupi District, Karnataka, India. *Geochemistry.* **2020**, *80*, 125647. [CrossRef]
9. Vallejos, A.; Daniele, L.; Sola, F.; Molina, L.; Pulido-Bosch, A. Anthropic-induced salinization in a dolomite coastal aquifer. Hydrogeochemical processes. *J. Geochem. Explor.* **2020**, *209*, 106438. [CrossRef]
10. Kazakis, N.; Pavlou, A.; Vargemezis, G.; Voudouris, K.S.; Soulios, G.; Pliakas, F.; Tsokas, G. Seawater intrusion mapping using electrical resistivity tomography and hydrochemical data. An application in the coastal area of eastern Thermaikos Gulf, Greece. *Sci. Total Environ.* **2016**, *543*, 373–387. [CrossRef]
11. Koffi, Y.P.; Meli'i, J.L.; Aretouyap, Z.; Gweth, M.M.A.; Fils, S.C.N.; Biringanine, G.N.; Oyoa, V.; Perilli, N.; Nouck, P.N. Possible pathways of seawater intrusion along the Mount-Cameroon coastal area using remote sensing and GIS techniques. *Adv. Space Res.* **2022**, *69*, 2047–2060. [CrossRef]
12. Nair, I.S.; Rajaveni, S.P.; Schneider, M.; Elango, L. Geochemical and isotopic signatures for the identification of seawater intrusion in an alluvial aquifer. *J. Earth Syst. Sci.* **2015**, *124*, 1281–1291. [CrossRef]

13. Tran, D.A.; Tsujimura, M.; Vo, L.P.; Nguyen, V.T.; Nguyen, L.D.; Dang, T.D. Stable isotope characteristics of water resources in the coastal area of the Vietnamese Mekong Delta. *Isot. Environ. Health Stud.* **2019**, *55*, 566–587. [CrossRef]

14. Xiao, Y.K.; Yin, D.Z.; Liu, W.G.; Wang, Q.Z.; Wei, H.Z. Boron isotope method for study of seawater intrusion. *Sci. China Ser. E-Technol. Sci.* **2001**, *44*, 62–71. [CrossRef]

15. Ma, Z.L.; Gao, L.; Sun, M.X.; Liao, Y.J.; Bai, S.J.; Wu, Z.J.; Li, J.T. Microbial diversity in groundwater and its response to seawater intrusion in Beihai City, Southern China. *Front. Microbiol.* **2022**, *13*, 876665. [CrossRef] [PubMed]

16. Pulido-Velazquez, D.; Baena-Ruiz, L.; Fernandes, J.; Arnó, G.; Hinsby, K.; Voutchkova, D.D.; Hansen, B.; Retike, I.; Bikse, J.; Collados-Lara, A.J.; et al. Assessment of chloride natural background levels by applying statistical approaches. Analyses of European coastal aquifers in different environments. *Mar. Pollut. Bull.* **2022**, *174*, 113303. [CrossRef] [PubMed]

17. Asare, A.; Appiah-Adjei, E.K.; Owusu-Nimo, F.; Ali, B. Lateral and vertical mapping of salinity along the coast of Ghana using Electrical Resistivity Tomography: The case of Central Region. *Results Geophys. Sci.* **2022**, *12*, 100048.

18. Xu, Z.L.; Tong, J.X.; Hu, B.X.; Yan, Z. Mapping and monitoring seasonal and tidal effects on the salt-freshwater interface using electrical resistivity tomography techniques. *Estuar. Coast. Shelf Sci.* **2022**, *276*, 108051. [CrossRef]

19. Han, D.M.; Kohfahl, C.; Song, X.F.; Xiao, G.Q.; Yang, J.L. Geochemical and isotopic evidence for palaeo-seawater intrusion into the south coast aquifer of Laizhou Bay, China. *Appl. Geochem.* **2011**, *26*, 863–883. [CrossRef]

20. Zhang, Z.; Yi, L.X.; Dong, Y.C.; Lv, T.X.; Zheng, Y.J. Application of radium isotopes to estimate seawater intrusion rate in coastal aquifers. *Appl. Geochem.* **2023**, *158*, 105816. [CrossRef]

21. Zhang, X.Y.; Qi, L.L.; Li, W.M.; Hu, B.X.; Dai, Z.X. Bacterial community variations with salinity in the saltwater-intruded estuarine aquifer. *Sci. Total Environ.* **2021**, *755*, 142423. [CrossRef] [PubMed]

22. Wang, J.J.; Yang, D.M.; Zhang, Y.; Shen, J.; van der Gast, C.; Hahn, M.W.; Wu, Q.L. Do patterns of bacterial diversity along salinity gradients differ from those observed for macroorganisms? *PLoS ONE* **2011**, *6*, e27597. [CrossRef]

23. Yang, J.; Ma, L.; Jiang, H.C.; Wu, G.; Dong, H.L. Salinity shapes microbial diversity and community structure in surface sediments of the Qinghai-Tibetan Lakes. *Sci. Rep.* **2016**, *6*, 25078. [CrossRef] [PubMed]

24. Adamou, H.; Ibrahim, B.; Salack, S.; Adamou, R.; Sanfo, S.; Liersch, S. Physico-chemical and bacteriological quality of groundwater in a rural area of Western Niger: A case study of Bonkoukou. *J. Water Health.* **2020**, *18*, 77–90. [CrossRef]

25. Li, B.; Wang, X.M.; Liu, G.; Zheng, L.F.; Cheng, C. Microbial diversity response to geochemical gradient characteristics on AMD from abandoned Dashu pyrite mine in Southwest China. *Environ. Sci. Pollut. Res.* **2022**, *29*, 74983–74997. [CrossRef] [PubMed]

26. Boano, F.; Demaria, A.; Revelli, R.; Ridolfi, L. Biogeochemical zonation due to intrameander hyporheic flow. *Water Resour. Res.* **2010**, *46*, W02511. [CrossRef]

27. Ding, D. Transport of bacteria in aquifer sediment: Experiments and modeling. *Hydrogeol. J.* **2010**, *18*, 669–679. [CrossRef]

28. Bao, P.; Li, G.X.; Sun, G.X.; Xu, Y.Y.; Meharg, A.A.; Zhu, Y.G. The role of sulfate-reducing prokaryotes in the coupling of element biogeochemical cycling. *Sci. Total Environ.* **2018**, *613*, 398–408. [CrossRef] [PubMed]

29. Li, P.; Tan, T.; Liu, H.; Wang, H.L. Functional microbial communities and the biogeochemical cycles in groundwater. *Acta Microbiol. Sin.* **2021**, *61*, 1598–1609.

30. Rogers, K.L.; Carreres-Calabuig, J.A.; Gorokh, E.; Posth, N.R. Micro-by-micro interactions: How microorganisms influence the fate of marine microplastics. *Limnol. Oceanogr. Lett.* **2020**, *5*, 18–36. [CrossRef]

31. Bradley, P.M. Microbial degradation of chloroethenes in groundwater systems. *Hydrogeol. J.* **2000**, *8*, 104–111. [CrossRef]

32. Bulatovic, S.; Maric, N.; Knudsen, T.S.; Avdalovic, J.; Ilic, M.; Ovancicevic, B.J.; Vrvic, M.M. Bioremediation of groundwater contaminated with petroleum hydrocarbons applied at a site in Belgrade (Serbia). *J. Serbian Chem. Soc.* **2020**, *85*, 1067–1081. [CrossRef]

33. Gaza, S.; Schmidt, K.R.; Weigold, P.; Heidinger, M.; Tiehm, A. Aerobic metabolic trichloroethene biodegradation under field-relevant conditions. *Water Res.* **2019**, *151*, 343–348. [CrossRef]

34. Chen, L.; Hu, B.X.; Dai, H.; Zhang, X.Y.; Xia, C.A.; Zhang, J. Characterizing microbial diversity and community composition of groundwater in a salt-freshwater transition zone. *Sci. Total Environ.* **2019**, *678*, 574–584. [CrossRef] [PubMed]

35. Chen, L.; Zhang, J.; Dai, H.; Hu, B.X.; Tong, J.X.; Gui, D.W.; Zhang, X.Y.; Xia, C.A. Comparison of the groundwater microbial community in a salt-freshwater mixing zone during the dry and wet seasons. *J. Environ. Manag.* **2020**, *271*, 110969. [CrossRef]

36. Ketabchi, H.; Jahangir, M.S. Influence of aquifer heterogeneity on sea level rise-induced seawater intrusion: A probabilistic approach. *J. Contam. Hydrol.* **2021**, *236*, 103753. [CrossRef]

37. Mehdizadeh, S.S.; Karamalipour, S.E.; Asoodeh, R. Sea level rise effect on seawater intrusion into layered coastal aquifers (simulation using dispersive and sharp-interface approaches). *Ocean. Coast. Manag.* **2017**, *138*, 11–18. [CrossRef]

38. Colombani, N.; Osti, A.; Volta, G.; Mastrocicco, M. Impact of Climate Change on Salinization of Coastal Water Resources. *Water Resour. Manag.* **2016**, *30*, 2483–2496. [CrossRef]

39. Ruffine, L.; Deusner, C.; Haeckel, M.; Kossel, E.; Toucanne, S.; Chéron, S.; Boissier, A.; Schmidt, M.; Donval, J.P.; Scholz, F.; et al. Effects of postglacial seawater intrusion on sediment geochemical characteristics in the Romanian sector of the Black Sea. *Mar. Pet. Geol.* **2021**, *123*, 104746. [CrossRef]

40. Selak, L.; Markovic, T.; Pjevac, P.; Orlic, S. Microbial marker for seawater intrusion in a coastal Mediterranean shallow Lake, Lake Vrana, Croatia. *Sci. Total Environ.* **2022**, *849* (Suppl. C), 157859. [CrossRef]

41. Tan, B.; Liu, C.; Tan, X.; You, X.J.; Dai, C.M.; Liu, S.G.; Li, J.; Li, N.W. Heavy metal transport driven by seawater-freshwater interface dynamics: The role of colloid mobilization and aquifer pore structure change. *Water Res.* **2022**, *217*, 118370. [CrossRef]

42. Karczewski, K.; Riss, H.W.; Meyer, E.I. Comparison of DNA-fingerprinting (T-RFLP) and high-throughput sequencing (HTS) to assess the diversity and composition of microbial communities in groundwater ecosystems. *Limnologica.* **2017**, *67*, 45–53. [CrossRef]

43. Sundberg, C.; Al-Soud, W.A.; Larsson, M.; Alm, E.; Yekta, S.S.; Svensson, B.H.; Sorensen, S.J.; Karlsson, A. 454 pyrosequencing analyses of bacterial and archaeal richness in 21 full-scale biogas digesters. *FEMS Microbiol. Ecol.* **2013**, *85*, 612–626. [CrossRef]

44. Caporaso, J.G.; Kuczynski, J.; Stombaugh, J.; Bittinger, K.; Bushman, F.D.; Costello, E.K.; Fierer, N.; Peña, A.G.; Goodrich, J.K.; Gordon, J.I.; et al. QIIME allows analysis of high-throughput community sequencing data. *Nat. Methods.* **2010**, *7*, 335–336. [CrossRef]

45. Meng, L.; Zuo, R.; Wang, J.S.; Yang, J.; Li, Q.; Chen, M.H. The spatial variations of correlation between microbial diversity and groundwater quality derived from a riverbank filtration site, northeast China. *Sci. Total Environ.* **2020**, *706*, 135855. [CrossRef]

46. Wu, M.X.J.; Wang, H.M.; Wang, W.Q.; Song, Y.Y.; Ma, L.Y.; Lu, X.L.; Wang, N.; Liu, C.Y. The impact of heavy rain event on groundwater microbial communities in Xikuangshan, Hunan Province, P.R. China. *J. Hydrol.* **2021**, *595*, 125674. [CrossRef]

47. Zhang, X.Y.; Hu, B.X.; Ren, H.J.; Zhang, J. Composition and functional diversity of microbial community across a mangrove-inhabited mudflat as revealed by 16S rDNA gene sequences. *Sci. Total Environ.* **2018**, *633*, 518–528. [CrossRef]

48. Zhang, H.S.; Cai, W.T.; Guo, F.; Bian, C.; Liu, F.D.; Zhang, L.; Liu, J.W.; Zhao, M. Microbial community composition and environmental response characteristics of typical brackish groundwater in the North China Plain. *China Geol.* **2023**, *6*, 383–394. [CrossRef]

49. Yang, L.; Chen, Q.; Wei, J.; Fan, T.T.; Kong, L.Y.; Long, T.; Zhang, S.T.; Deng, S.P. Response of microbial communities in aquifers with multiple organic solvent contamination: Implications for MNA remedy. *J. Hazard. Mater.* **2024**, *474*, 134798. [CrossRef]

50. Langille, M.G.I.; Zaneveld, J.; Caporaso, J.G.; McDonald, D.; Knights, D.; Reyes, J.A.; Clemente, J.C.; Burkepile, D.E.; Thurber, R.L.V.; Knight, R. Predictive functional profiling of microbial communities using 16S rRNA marker gene sequences. *Nat. Biotechnol.* **2013**, *31*, 814–821. [CrossRef]

51. Chen, H.H.; Ma, K.Y.; Huang, Y.; Fu, Q.; Qiu, Y.B.; Yao, Z.Y. Significant response of microbial community to increased salinity across wetland ecosystems. *Geoderma.* **2022**, *415*, 115778. [CrossRef]

52. Zhou, Z.C.; Meng, H.; Gu, W.J.; Li, J.; Deng, M.C.; Gu, J.D. High-throughput sequencing reveals the main drivers of niche-differentiation of bacterial community in the surface sediments of the northern South China sea. *Mar. Environ. Res.* **2022**, *178*, 105641. [CrossRef]

53. Rocca, J.D.; Simonin, M.; Bernhardt, E.S.; Washburne, A.D.; Wright, J.P. Rare microbial taxa emerge when communities collide: Freshwater and marine microbiome responses to experimental mixing. *Ecology.* **2019**, *101*, e02956. [CrossRef]

54. Rath, K.M.; Fierer, N.; Murphy, D.V.; Rousk, J. Linking bacterial community composition to soil salinity along environmental gradients. *ISME J.* **2019**, *13*, 836–846. [CrossRef]

55. Héry, M.; Volant, A.; Garing, C.; Luquot, L.; Poulichet, F.E.; Gouze, P. Diversity and geochemical structuring of bacterial communities along a salinity gradient in a carbonate aquifer subject to seawater intrusion. *FEMS Microbiol. Ecol.* **2014**, *90*, 922–934. [CrossRef]

56. Yu, H.; Feng, S.; Qiu, H.; Liu, J.Y. Interaction between the hydrochemical environment, dissolved organic matter, and microbial communities in groundwater: A case study of a vegetable cultivation area in Huaibei Plain, China. *Sci. Total Environ.* **2023**, *895*, 165166. [CrossRef]

57. Wu, Q.L.; Zwart, G.; Schauer, M.; Kamst-van Agterveld, M.P.; Hahn, M.W. Bacterioplankton community composition along a salinity gradient of sixteen high-mountain lakes located on the Tibetan Plateau, China. *Appl. Environ. Microbiol.* **2006**, *72*, 5478–5485. [CrossRef]

58. Zhong, Z.P.; Liu, Y.; Miao, L.L.; Wang, F.; Chu, L.M.; Wang, J.L.; Liu, Z.P. Prokaryotic Community Structure Driven by Salinity and Ionic Concentrations in Plateau Lakes of the Tibetan Plateau. *Appl. Environ. Microbiol.* **2016**, *82*, 1846–1858. [CrossRef]

59. Kurtbke, D.I.; Okazaki, T.; Vobis, G.; Kim, S. *Actinobacteria in Marine Environments*; John Wiley & Sons, Ltd.: Hoboken, NJ, USA, 2020.

60. Liu, K.; Jiao, J.J.; Gu, J.D. Investigation on bacterial community and diversity in the multilayer aquifer-aquitard system of the Pearl River Delta, China. *Ecotoxicology* **2014**, *23*, 2041–2052. [CrossRef]

61. Chen, L.J.; Li, C.S.; Feng, Q.; Wei, Y.P.; Zheng, H.; Zhao, Y.; Feng, Y.J.; Li, H.Y. Shifts in soil microbial metabolic activities and community structures along a salinity gradient of irrigation water in a typical arid region of China. *Sci. Total Environ.* **2017**, *598*, 64–70. [CrossRef]

62. Kirchman, D.L.; Dittel, A.I.; Malmstrom, R.R.; Cottrell, M.T. Biogeography of major bacterial groups in the Delaware Estuary. *Limnol. Oceanogr.* **2005**, *50*, 1697–1706. [CrossRef]

63. Liu, J.W.; Yang, H.M.; Zhao, M.X.; Zhang, X.H. Spatial distribution patterns of benthic microbial communities along the Pearl Estuary, China. *Syst. Appl. Microbiol.* **2014**, *37*, 578–589. [CrossRef]

64. Campbell, B.J.; Kirchman, D.L. Bacterial diversity, community structure and potential growth rates along an estuarine salinity gradient. *ISME J.* **2013**, *7*, 210–220. [CrossRef]

65. Suh, S.S.; Park, M.; Hwang, J.; Kil, E.J.; Jung, S.W.; Lee, S.; Lee, T.K. Seasonal Dynamics of Marine Microbial Community in the South Sea of Korea. *PLoS ONE* **2015**, *10*, e0131633. [CrossRef]

66. Teeling, H.; Fuchs, B.M.; Becher, D.; Klockow, C.; Gardebrecht, A.; Bennke, C.M.; Kassabgy, M.; Huang, S.X.; Mann, A.J.; Waldmann, J.; et al. Substrate-Controlled Succession of Marine Bacterioplankton Populations Induced by a Phytoplankton Bloom. *Science* **2012**, *336*, 608–611. [CrossRef]

67. Unno, T.; Kim, J.; Kim, Y.; Nguyen, S.G.; Guevarra, R.B.; Kim, G.P.; Lee, J.H.; Sadowsky, M.J. Influence of seawater intrusion on microbial communities in groundwater. *Sci. Total Environ.* **2015**, *532*, 337–343. [CrossRef]

68. Hwang, C.Y.; Cho, B.C. Cohaesibacter gelatinilyticus gen. nov., sp nov., a marine bacterium that forms a distinct branch in the order Rhizobiales, and proposal of Cohaesibacteraceae fam. nov. *Int. J. Syst. Evol. Microbiol.* **2008**, *58*, 267–277. [CrossRef] [PubMed]

69. Gallego, S.; Vila, J.; Nieto, J.M.; Urdiain, M.; Rosselló-Móra, R.; Grifolla, M. Breoghania corrubedonensis gen. nov sp nov., a novel alphaproteobacterium isolated from a Galician beach (NW Spain) after the Prestige fuel oil spill, and emended description of the family Cohaesibacteraceae and the species Cohaesibacter gelatinilyticus. *Syst. Appl. Microbiol.* **2010**, *33*, 316–321. [CrossRef]

70. Zeiner, I.; Suul, J.A.; Marcos, A.; Molinas, M. System design and load profile shaping for a reverse osmosis desalination plant powered by a stand-alone PV system in Pozo Colorado, Paraguay. In Proceedings of the 9th International Conference on Ecological Vehicles and Renewable Energies (EVER), Monte Carlo, Monaco, 25–27 March 2014.

71. Yang, C.; Lv, D.T.; Jiang, S.Y.; Lin, H.; Sun, J.Q.; Li, K.J.; Sun, J. Soil salinity regulation of soil microbial carbon metabolic function in the Yellow River Delta, China. *Sci. Total Environ.* **2021**, *790*, 148258. [CrossRef] [PubMed]

72. Eloe, E.A.; Fadrosh, D.W.; Novotny, M.; Allen, L.Z.; Kim, M.; Lombardo, M.J.; Yee-Greenbaum, J.; Yooseph, S.; Allen, E.E.; Lasken, R.; et al. Going deeper: Metagenome of a hadopelagic microbial community. *PLoS ONE* **2011**, *6*, e20388. [CrossRef]

73. Sonawane, J.M.; Rai, A.K.; Sharma, M.; Tripathi, M.; Prasad, R. Microbial biofilms: Recent advances and progress in environmental bioremediation. *Sci. Total Environ.* **2022**, *824*, 153843. [CrossRef] [PubMed]

74. Liu, M.T.; Li, Q.L.; Sun, H.H.; Jia, S.Y.; He, X.W.; Li, M.; Zhang, X.X.; Ye, L. Impact of salinity on antibiotic resistance genes in wastewater treatment bioreactors. *Chem. Eng. J.* **2018**, *338*, 557–563. [CrossRef]

75. Yu, X.; Zhang, Y.; Tan, L.; Han, C.L.; Li, H.X.; Zhai, L.F.; Ma, W.Q.; Li, C.T.; Lu, X.Q. Microplastisphere may induce the enrichment of antibiotic resistance genes on microplastics in aquatic environments: A review. *Environ. Pollut.* **2022**, *310*, 119891. [CrossRef] [PubMed]

76. Zhao, Z.; Zhang, K.; Wu, N.; Li, W.J.; Xu, W.A.; Zhang, Y.; Niu, Z.G. Estuarine sediments are key hotspots of intracellular and extracellular antibiotic resistance genes: A high-throughput analysis in Haihe Estuary in China. *Environ. Int.* **2020**, *135*, 105385. [CrossRef] [PubMed]

77. Nishida, A.; Nakagawa, M.; Yamamura, M. Determinism of microbial community assembly by drastic environmental change. *PLoS ONE* **2021**, *16*, e0260591. [CrossRef] [PubMed]

78. Pellegrinetti, T.A.; Cotta, S.R.; Sarmento, H.; Costa, J.S.; Delbaje, E.; Montes, C.R.; Camargo, P.B.; Barbiero, L.; Rezende, A.T.; Fiore, M.F. Bacterial communities along environmental gradients in Tropical Soda Lakes. *Microb. Ecol.* **2022**, *85*, 892–903. [CrossRef] [PubMed]

79. Fu, Y.; Keats, K.F.; Rivkin, R.B.; Lang, A.S. Water mass and depth determine the distribution and diversity of Rhodobacterales in an Arctic marine system. *FEMS Microbiol. Ecol.* **2013**, *84*, 564–576. [CrossRef]

80. Giebel, H.A.; Brinkhoff, T.; Zwisler, W.; Selje, N.; Simon, M. Distribution of Roseobacter RCA and SAR11 lineages and distinct bacterial communities from the subtropics to the Southern Ocean. *Environ. Microbiol.* **2009**, *11*, 2164–2178. [CrossRef] [PubMed]

81. Chen, S.; He, Y.B.; Xie, Z.X.; Kong, L.F.; Yan, K.Q.; Li, D.X.; Wu, P.F.; Zheng, R.W.; Peng, L.; Chen, J.W.; et al. Metaproteomics reveals nutrient availability shaping distinct microbial community and metabolic niche in the nutrient-depleted and replete layers of an oligotrophic euphotic zone. *Sci. Total Environ.* **2021**, *774*, 145123. [CrossRef]

82. Gilbert, J.A.; Steele, J.A.; Caporaso, J.G.; Steinbrueck, L.; Reeder, J.; Temperton, B.; Huse, S.; McHardy, A.C.; Knight, R.; Joint, I.; et al. Defining seasonal marine microbial community dynamics. *ISME J.* **2012**, *6*, 298–308. [CrossRef]

83. Paver, S.F.; Muratore, D.; Newton, R.J.; Coleman, M.L. Re-evaluating the salty divide: Phylogenetic specificity of transitions between marine and freshwater systems. *Cold Spring Harb. Lab.* **2018**, *3*, e00232-18.

84. Liu, S.J.; Moon, C.D.; Zheng, N.; Huws, S.R.; Zhao, S.G.; Wang, J.Q. Opportunities and challenges of using metagenomic data to bring uncultured microbes into cultivation. *Microbiome* **2022**, *10*, 1–14. [CrossRef] [PubMed]

85. Koskella, B.; Hall, L.J.; Metcalf, C.J.E. The microbiome beyond the horizon of ecological and evolutionary theory. *Nat. Ecol. Evol.* **2017**, *1*, 1606–1615. [CrossRef] [PubMed]

86. Babajanyan, S.G.; Garushyants, S.K.; Wolf, Y.I.; Koonin, E.V. Microbial diversity and ecological complexity emerging from environmental variation and horizontal gene transfer in a simple mathematical model. *BMC Biol.* **2024**, *22*, 148. [CrossRef]